

AN INTEGRATED APPROACH TO EVALUATING SOIL COMPACTION: THE IMPACT OF SHEAR BANDS IN NON-PNEUMATIC TIRES

*Juthanee Phromjan¹, Kittipos Loksupapaiboon², Panit Kamma³ and Chakrit Suvanjumrat⁴

¹Department of Mechanical Engineering, Faculty of Engineering, King Mongkut's University of Technology Thonburi, Thailand; ²Department of Maritime Engineering, Faculty of International Maritime Studies, Kasetsart University Sriracha Campus, Thailand; ³Department of Mechanical and Manufacturing Engineering, Faculty of Science and Engineering, Kasetsart University Chalermpkrakiat Sakon Nakhon Province Campus, Thailand;

⁴Department of Mechanical Engineering, Faculty of Engineering, Mahidol University, Thailand

*Corresponding Author, Received: 19 Dec. 2024, Revised: 22 Jan. 2025, Accepted: 27 Jan. 2025

ABSTRACT: This study investigated the effects of non-pneumatic tires (NPTs) on soil compaction, emphasizing the role of shear bands in influencing vertical stiffness and soil bulk density (BD). By combining finite element analysis with semi-empirical modeling, the research provided a detailed assessment of NPT behavior under various design configurations. The results demonstrated significant variations in vertical stiffness and BD across different NPT designs, driven by factors such as the number and alignment of belt layers. Group A NPTs exhibited vertical stiffness levels that were intermediate between those of agricultural tires and pneumatic tires (PTs) of comparable size. Among these, the M4-4 configuration achieved a notable reduction in BD, indicating its potential effectiveness in minimizing soil compaction. Conversely, Group B NPTs displayed higher vertical stiffness than PTs, with the M3-6 configuration particularly effective in reducing BD despite its increased stiffness. These findings highlight the intricate relationship between NPT design parameters and their impact on soil properties. The research contributed to a deeper understanding of how NPT configurations influence both vertical stiffness and soil compaction, providing valuable insights for optimizing tire designs in agricultural applications.

Keywords: Agriculture, Finite Element Method, Non-Pneumatic Tire, Shear Band, Soil Compaction

1. INTRODUCTION

Soil compaction is a critical issue in modern agriculture, posing significant challenges to soil health, crop productivity, and overall ecosystem balance [1]. Compacted soils adversely impact soil structure, reducing porosity and aeration while also impeding root penetration and water infiltration. This limits nutrient availability for plants, leading to reduced agricultural yields and contributing to environmental degradation [2-5]. Such effects highlight the urgent need for effective strategies to mitigate soil compaction and sustain agricultural productivity.

The widespread use of agricultural machinery is a primary factor contributing to soil compaction [6-8]. While this machinery is essential for meeting high productivity demands, the pressure it exerts compresses soil layers, disrupting their natural composition and functionality. Current approaches to addressing this issue include the use of low-inflation pressure tires, which increase the contact area between the tire and soil, thereby reducing surface deformation and stress concentration [9]. However, these tires often face durability issues, as they are prone to damage in demanding field conditions, limiting their long-term utility [10].

In response to these challenges, non-pneumatic

tires (NPTs) have gained attention as a potential solution. Their unique structural characteristics, including their resistance to damage and adaptability to diverse applications, make them particularly promising for agricultural machinery and off-road vehicles [11-14]. The spoke structure of NPTs has shown the potential to reduce soil compaction by distributing loads more effectively [15, 16]. Additionally, NPTs are puncture-proof, eliminating the risk of air leaks and reducing maintenance requirements, which is a critical advantage in rugged and remote environments. Their durability and ability to maintain performance under extreme conditions further enhance their suitability for heavy-duty applications. Another key feature of NPTs is the shear band, a critical component that directly influences tire characteristics and load distribution to the ground. It has been found that the thickness of the belt layers in the shear band significantly impacts the NPTs' strength, while their positioning affects the footprint between the NPTs and the ground. Therefore, the shear band's thickness, geometry, and alignment significantly affect tire performance and its impact on soil compaction [17, 18].

Despite these promising features, the mechanisms through which NPTs influence soil compaction remain insufficiently understood. Specifically, the role of shear bands in shaping the soil's response to

applied loads requires further investigation. Understanding these dynamics is essential for optimizing NPT designs to achieve reduced soil compaction while maintaining high performance in agricultural settings.

This study employs an integrated research approach to address these knowledge gaps. By combining semi-empirical testing with advanced numerical modeling techniques, the research provides a detailed analysis of the interactions between NPTs and soil. Controlled laboratory experiments were conducted under varied conditions to simulate real-world scenarios, and the findings were validated using finite element models. This comprehensive methodology aims to unravel the complex relationships between NPT structural features, such as shear bands, and their effects on soil compaction. A key innovation lies in investigating how shear band geometry influences soil behavior under compression conditions, a topic previously underexplored. The insights gained from this study are expected to inform the development of NPT designs tailored for agricultural applications, contributing to improved efficiency, reduced environmental impact, and sustainable farming practices.

2. RESEARCH SIGNIFICANCE

The outcomes are expected to contribute to a comprehensive understanding of the soil compaction mechanisms induced by NPTs, with a particular emphasis on the role of shear bands by integrating semi-empirical and numerical modeling. The findings offer actionable recommendations for optimizing shear band geometry, enabling the tire industry to develop NPTs specifically designed for agricultural needs. Furthermore, these insights can inform the selection and deployment of NPT-equipped machinery, reducing soil degradation and improving crop yields. By mitigating soil compaction, these advancements support long-term soil health, enhance productivity, and contribute to more sustainable farming practices.

3. SEMI-EMPIRICAL MODEL

Empirical or semi-empirical models have been developed since 1913 to study the interaction between structure and soil. The relationship between pressure and sinkage as written in Eq. (1) was proposed and widely used when the soil is assumed to be homogeneous. Moreover, when slip does not occur and the vertical acceleration of the pressure source is negligible, the pressure source was considered to have moved steadily.

$$p = kZ^m \quad (1)$$

where p is the pressure, k is the sinkage modulus,

Z is the soil sinkage, the distance from the lowest point of the track to the undisturbed soil surface, and m is the sinkage exponent.

Later, the sinkage modulus was separated into two parts, and the relationship was rewritten as shown in Eq. (2). The effect of the pressure source size has also been considered [19].

$$p = \left(\frac{k_c}{b} + k_\phi \right) Z^m \quad (2)$$

where k_c is the sinkage modulus influenced by the soil cohesion, k_ϕ denotes the sinkage modulus influenced by the soil friction angle, and b is the smaller dimension of the contact patch.

3.1 Pressure-Sinkage Relationship

To obtain the model's constants, plunger testing was performed by the tire-soil compression machine in a laboratory scale under the controlled conditions [15, 16]. The testing soil was classified as a Sandy Clay Loam (SCL) soil with 13% silt, 64% sand, and 23% clay. This soil type is suitable for field crops such as sugarcane, maize, and cassava [20, 21]. Since, this soil type creates a stable structure that ensures proper aeration, retains water effectively, and helps maintain a moderate soil temperature. The soil density and moisture content were prepared at 0.89 Mg/m³ and 15% w/w, respectively, which are adequate for plant growth. Two sizes of cylinder plungers were then pressed on the soil surface with controlled displacement under the same conditions. The applied load was investigated by a load cell which had an accuracy of 6.92%. The pressure curves were then produced for each plunger. Lastly, the pressure-sinkage relationship was proposed as expressed in Eq. (3), and the soil sinkage was calculated using Eq. (4), where sinkage is in millimeters (mm) and pressure is in Pascals (Pa).

$$p = \left(\frac{2,121,899}{b} - 2,830.991 \right) Z^{0.93} \quad (3)$$

$$Z = \left(\frac{p}{2,121,899/b - 2,830.991} \right)^{1/0.93}, \text{ mm} \quad (4)$$

4. FINITE ELEMENT METHOD

The finite element method (FEM) was used to model the NPT characteristics necessary for the integration. The NPT model was created according to the TWEEL 12N16.5 ALL-TERRAIN, developed by Michelin. The shell element was used to create the

spoke elements, while the others were made of hexahedral element. The NPT model was compressed by a rigid flat plate according to the tire stiffness testing, as presented in Fig. 1. The contact patch characteristics were obtained from the finite element analysis (FEA). The material properties of the NPT model can be classified into three main types: 1) rubber for the tread and wall, 2) polyurethane (PU) for the spoke structure, and 3) steel for the belt layers. The Mooney-Rivlin constitutive model was used to describe the deformation characteristics of the first two material types, with the model constants presented in Table 1. The steel was characterized by elastic material properties, with a Young's modulus of 200 GPa and a Poisson's ratio of 0.3. The details of the boundary conditions and material properties were additionally described in previous works [15, 20]. The model's validity was confirmed.

Table 1 The constants of the hyperelastic material properties

Components	C_{10} (MPa)	C_{01} (MPa)	K (MPa)
Tread and Wall	1.19085	0	9,670.24
Spoke structure	0.5063	4.2552	42,449.00

In this research, the effects of the NPT's shear band on soil compaction were studied. The shear band is a composite structure originally consisting of four steel belt layers in the rubber wall, as presented in Fig. 2(a). Similarly, the finite element (FE) model of the shear band was created according to this sequence, as shown in Fig. 2(b). The thicknesses of the belt layers were 3, 1, 1, and 2 mm for layers 1 to 4, respectively, with the first layer located next to the tire tread according to the shear band geometry of the TWEEL NPT. The features of the inserted belt layers were then varied as described in Table 2, while the other components of the NPT remained the same. Once all possibilities were captured, they were grouped into five categories with a total of 16 models. The weights of the shear bands were collected for further comparison.

All models were then vertically pressed with a compression force (F) of 4,750 N, which is the

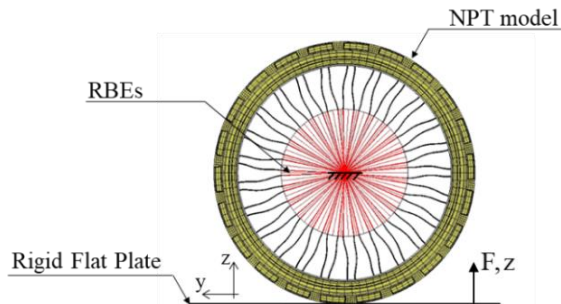


Fig.1 The boundary conditions of the compressed NPT model

maximum load under consideration for a small tractor [21]. The simulation results for each case study group are presented in Fig. 3. The response of the NPTs under compression load was first collected in terms of the load-deformation relationship.

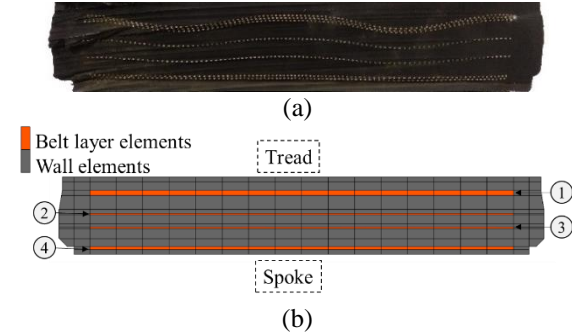


Fig.2 The cross-section of (a) the actual shear band and (b) the shear band model of the prototype NPT

Table 2 The description of the FE models

Model	Existence of the belt layer(s)	Weight of the shear band (kg)	Vertical stiffness (N/mm)	Safety factor of spokes
Group 1: 4 belt layers (Original)				
M1-1	1 2 3 4	72.30	798.40	21.54
Group 2: 3 belt layers				
M2-1	2 3 4	59.50	665.59	19.41
M2-2	1 3 4	68.17	758.35	20.40
M2-3	1 2 4	68.41	758.95	20.40
M2-4	1 2 3	64.58	716.08	20.04
Group 3: 2 belt layers				
M3-1	1 2	60.60	673.49	19.66
M3-2	1 3	60.37	681.92	19.77
M3-3	2 3	51.69	556.26	16.61
M3-4	3 4	55.29	613.38	18.12
M3-5	2 4	55.53	628.75	18.30
M3-6	1 4	64.20	731.71	20.24
Group 4: 1 belt layer				
M4-1	1	56.39	615.94	17.81
M4-2	2	47.72	459.82	14.95
M4-3	3	47.48	458.39	14.96
M4-4	4	51.31	547.81	16.50
Group 5: no belt layer				
M5-1	-	43.51	88.42	5.40

The vertical stiffness resulting from dividing the compression force (F) by the tire deformation was then evaluated, as presented in Table 2. The validation case (M1-1) had an error of 5.11% when compared to the experiment as shown in Fig. 4. The vertical stiffnesses of the same-size conventional pneumatic tire (PT) and agricultural tire (size 8.3-20)

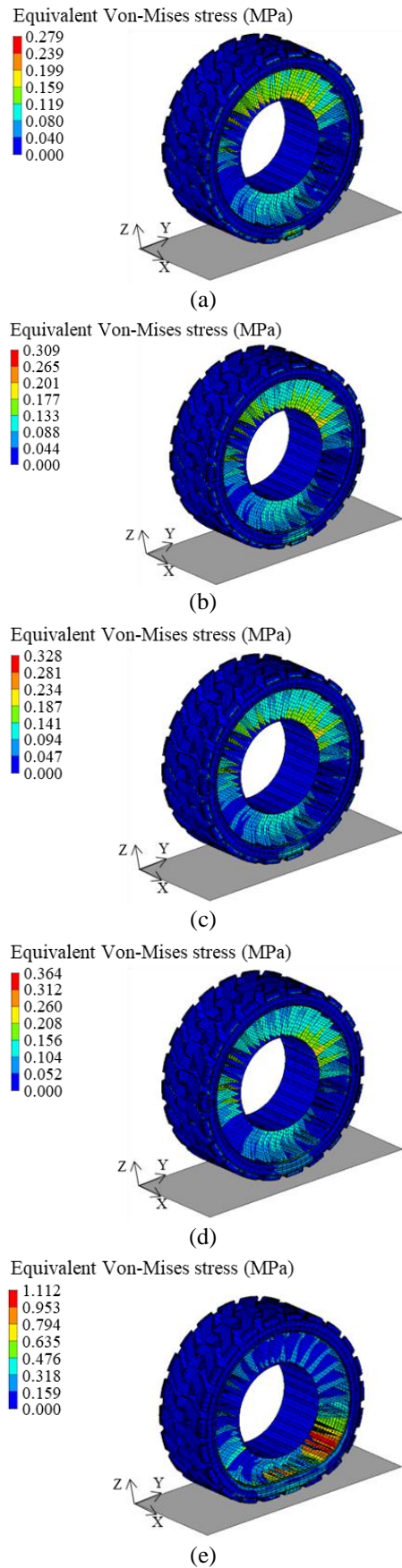


Fig.3 Deformation and stress contour of (a) M1-1, (b) M2-1, (c) M3-5, (d) M4-4, and (e) M5-1 models

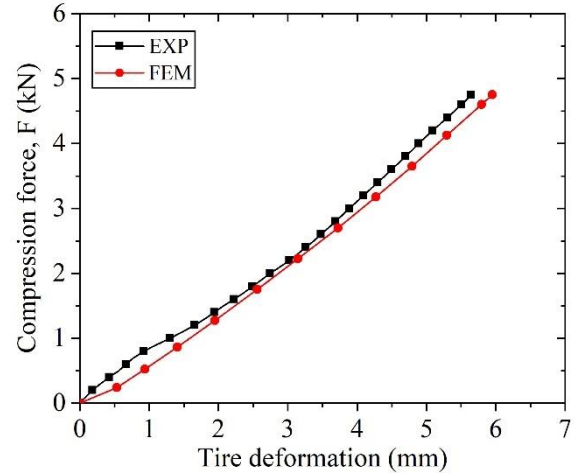


Fig.4 Comparison result of the compressed NPT under compressive load of 4,750 N

were 658.17 N/mm and 316.91 N/mm, respectively [15]. The simulation results revealed that the presence of belt layers played a critical role in influencing the performance of NPTs. When all belt layers were removed from the tire structure, the NPT exhibited significant deformation, as illustrated in Fig. 3. This finding highlights the structural importance of the belt layers in maintaining the tire's overall stability and integrity under load. Across all analyzed models, the deformation characteristics of the NPTs followed a consistent trend, with one notable exception: the M5-1 model. The maximum stress was observed to occur in the spoke elements located within the support region of the spoke structure. In this region, the spokes were primarily subjected to tension, indicating a distinct loading behavior, as reported in [20].

Moreover, the local stress occurring on the spokes could be observed via the color contour. The maximum stress tended to increase with decreasing number of the belt layers. The safety factor of the spoke was then evaluated, considering the yield stress of the polyurethane (PU) used for the spoke structure, which was 6 MPa. When comparing between groups, the number of belt layers significantly affected the NPT's vertical stiffness, which decreased as the number of belt layers was reduced. Unfortunately, the NPT without the belt layers could not maintain the proper characteristics in terms of both vertical stiffness and safety factor as shown in Fig. 3(e). However, the NPT with only one layer still had a higher vertical stiffness than the agricultural tire of equivalent size, although it was lower than the vertical stiffness of the same-size PT. When considering within groups, it was found that the presence of belt layer number 1 provided high vertical stiffness due to its being the thickest layer. Similarly, the thin layers (layers 2 and 3) had less effect on the durability of the NPTs. Meanwhile, another influence that could be observed was the belt layer alignment. This was clearly seen in the comparison between M3-

4 and M3-5. Even though layers 2 and 3 are of the same thickness, positioning the belt layer closer to the tread results in higher vertical stiffness. The safety factor of the spoke structure was also related to the tire's vertical stiffness. However, lower vertical stiffness meant a lighter shear band, which implies the possibility of lower resource consumption.

The simulation results provided essential information regarding the tire footprint, which is a critical factor in studying the behavior and characteristics of the contact patch. Understanding these characteristics is fundamental for evaluating the performance of the tires in various applications, particularly when examining their interaction with different surfaces. The analysis indicated that the belt layers in the tire structure played a pivotal role in shaping the contact behavior. Their presence had a significant influence on the distribution and dynamics of the contact patch, which in turn has direct implications for soil compaction. Figure 5 visually compares the contact patch obtained through FEA for the original configuration of the NPT and a modified version where the belt layers were removed. The comparison clearly highlights the impact of the belt layers on the contact patch geometry. Furthermore, an interesting finding from the simulation revealed that, for NPTs, the smaller dimension of the contact patch was not necessarily its width. This observation contrasts with the behavior typically observed in pneumatic tires [22].

5. INTEGRATION APPROACH

The proposed integration approach was developed by synthesizing the outcomes of FEA with a semi-empirical model [15, 16, 23]. This methodology enabled a comprehensive evaluation by incorporating simulation data into analytical modeling. Specifically, the unknown variables associated with the pressure-sinkage relationship, as defined in Eq. (4), could be substituted with parameters either obtained directly from the simulation results or calculated based on them. In this study, advanced image processing techniques were employed using MATLAB software to accurately segment the contact patch from the non-contact zone, as depicted in Fig. 6.

MATLAB's user-friendly interface and fast processing capabilities make it ideal for analyzing complex structures. Its customizable tools enable precise segmentation and boundary identification. Following this, key contact patch characteristics, such as the width and length of the contact patch, along with the overall contact area (CA), were analyzed using CAD software. Finally, the mean contact pressure was determined by calculating the ratio of the compressive force exerted by the tire to the measured contact area, as outlined in Eq. (5). This process provided a quantitative assessment of the

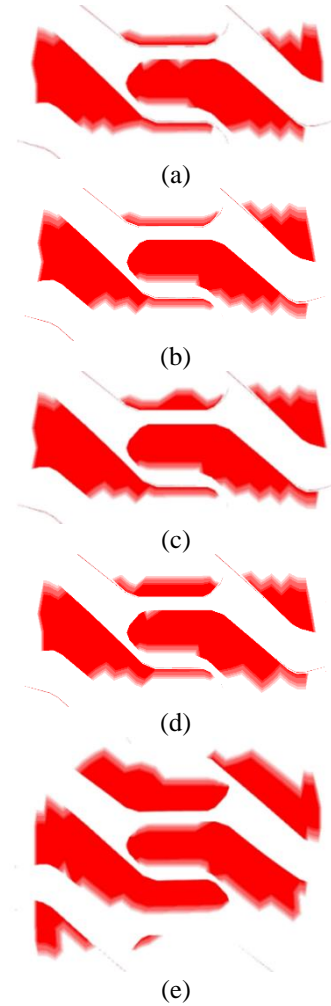


Fig.5 Footprints of (a) M1-1, (b) M2-1, (c) M3-5, (d) M4-4 and (e) M5-1 models

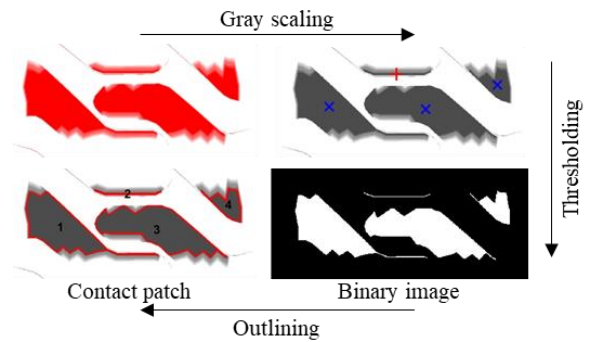


Fig.6 The contact patch segmentation process

$$p = \frac{F}{CA}, \text{ Pa} \quad (5)$$

pressure distribution.

The predicted soil sinkage of the original case was further compared to the experimental results, which were described in detail in previous work [15]. The developed tire-soil compression machine was utilized in combination with a portable 3D scanner. The compression load ranged from 3,550 to 4,750 N, with

intervals of 600 N. The comparison results are presented in Table 3. The validity was acceptable, with an average error of 12.91%. The difficulty in controlling soil conditions might have contributed to the uncertainties and errors in the experiment. This approach was then utilized to investigate the effects of shear bands on soil compaction. Moreover, the soil bulk density of the compressed soil surface was further experimentally investigated, as also presented in Table 3. Soil bulk density increased with the increase in soil sinkage. Their relationship is polynomial, as expressed by Eq. (6), with an R^2 value of 0.83 and adjusted R^2 value of 0.92. The limitation of the analyzed soil depth is a maximum of 250 mm, due to the experimental setup conditions.

$$BD = 0.0009Z^2 - 0.0045Z + 0.89, \text{ Mg/m}^3 \quad (6)$$

Table 3 The validation results of the approach

Compression force, F (N)	Soil bulk density (Mg/m ³)	Soil sinkage, Z (mm)	
		Experiment	Predicted
3,550	1.055	15.8	17.23
4,150	1.077	18.0	20.24
4,750	1.155	19.3	22.63

Table 4 presents all investigated results calculated using the validated integrated approach. An ANOVA test was further performed, revealing that NPTs in groups 2-4 showed significant differences in terms of CA, with a P-value lower than 0.1 when using a significance level (α) of 0.1 due to the small sample size. However, the P-value was much lower than 0.05 when all cases were compared together.

6. EFFECTS OF SHEAR BANDS ON SOIL COMPACTION

The changed soil bulk density, influenced by various NPTs, was further calculated using Eq. (6), and the prediction results were presented in Fig. 7. Soil bulk density is a sensitive value, where even the slightest change can impact plant growth [24]. A soil bulk density of 1.3 Mg/m³ or less is suitable for plant growth, while the range between 1.3 and 1.55 Mg/m³ is considered fair. Exceeding 1.8 Mg/m³ is critical for plant growth. Therefore, changes in soil bulk density must be carefully considered. It was found that in group 2-4, there was a significant difference in terms of Z and BD with a p-value lower than 0.1. Likewise, it was much lower than 0.05 when all cases were compared together. The results revealed that the number and alignment of the belt layers in the shear band significantly affected soil compaction.

However, this effect did not change in accordance with the trend of vertical stiffness but rather inversely changed with the trend of CA. This phenomenon was observed in case M5-1, which had the weakest

Table 4 The evaluation results

Model	b (mm)	CA (cm ²)	p (kPa)	Z (mm)
M1-1	107.85	155.05	306.35	22.63
M2-1	110.89	161.50	294.12	22.43
M2-2	110.03	159.55	297.72	22.50
M2-3	110.17	160.19	296.52	22.44
M2-4	110.36	160.64	295.69	22.42
M3-1	110.31	158.64	299.43	22.71
M3-2	110.38	159.51	297.80	22.60
M3-3	109.37	169.83	279.69	20.88
M3-4	109.89	175.22	271.09	20.31
M3-5	109.88	170.06	279.31	20.97
M3-6	110.36	163.00	291.42	22.07
M4-1	110.44	160.34	296.45	22.49
M4-2	109.54	172.61	275.18	20.56
M4-3	108.92	176.07	269.79	19.98
M4-4	109.29	179.79	264.19	19.62
M5-1	199.74	265.82	178.69	29.03

stiffness but yielded the highest BD. Similarly, it was found that the results did not follow the same trend in each studied parameter when considered separately in groups. Consequently, it can be concluded that the effect of shear band characteristics on soil compaction is too complex to be deeply understood with traditional methods, as these effects are influenced by a combination of various parameters. Therefore, effective design or development of this part may require advanced methods such as artificial neural networks (ANN).

Fortunately, the findings from this research offer valuable insights and alternatives for the development of NPTs tailored for agricultural tractors. By considering both vertical stiffness and BD as evaluation criteria, the study established benchmarks based on the vertical stiffness of a same-size PT and an agricultural tire. It was observed that, except for the M5-1 configuration, all NPT cases exhibited higher vertical stiffness than the agricultural tire. However, only eight cases demonstrated higher vertical stiffness than the same-size PT. Based on these results, the configurations were further categorized into two distinct groups, as illustrated in Figure 7. Group A included cases M3-3, M3-4, M3-5, and M4-1 through M4-4, which had vertical stiffness levels falling between the two benchmarks. Among these, if minimizing BD was the primary goal, the M4-4 configuration emerged as the optimal choice. This design achieved a reduction in vertical stiffness of approximately 29.49% and a decrease in BD of 8.07% compared to the original case (M1-1).

Group B consisted of the remaining configurations, all of which had vertical stiffness values exceeding that of the same-size PT. Within this group, the M3-6 model was particularly noteworthy,

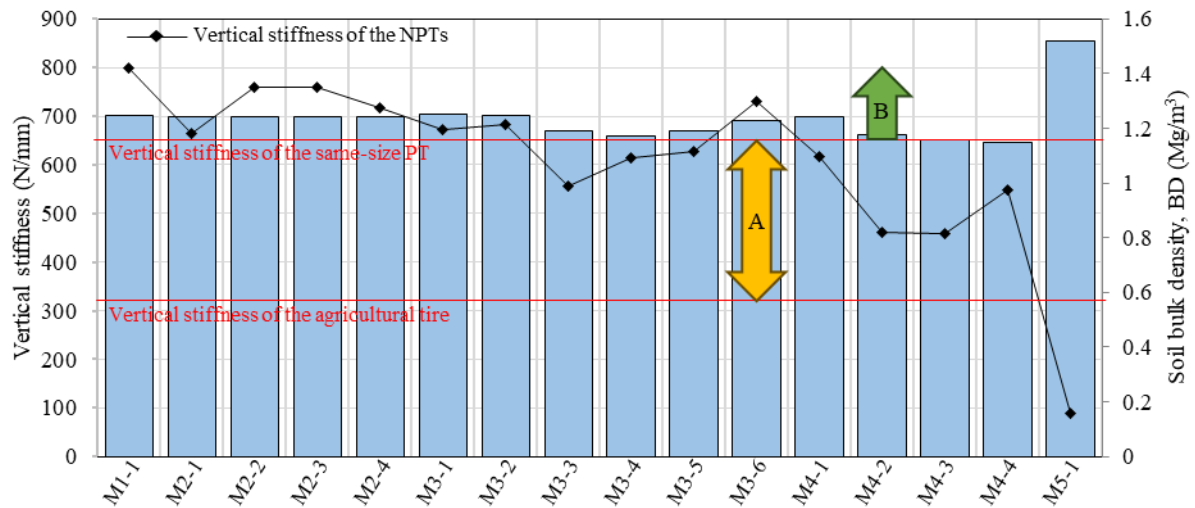


Fig.7 The predicted soil bulk density under compression by the NPTs (in bar graph) analyzed in relation to the tire's vertical stiffness

achieving a reduction in vertical stiffness of 7.86% and a decrease in BD of 1.58% relative to the original case. Nevertheless, the study emphasizes that other configurations within both groups could be selected to meet specific performance requirements, allowing for tailored solutions based on the desired balance between vertical stiffness and soil compaction.

7. CONCLUSIONS

This research investigated the impact of non-pneumatic tires on soil compaction, with a particular focus on understanding how shear bands affect vertical stiffness and soil bulk density. By integrating finite element analysis with semi-empirical modeling in the laboratory scale, the study provided a detailed and comprehensive perspective on the behavior of NPTs under various configurations under the specified conditions.

The results demonstrated significant differences in both vertical stiffness and BD across different NPT designs. Key factors influencing these variations included the number of belt layers and their alignment. NPTs in Group A exhibited vertical stiffness levels that were intermediate between those of agricultural tires and pneumatic tires (PTs) of the same size. Among these, the M4-4 configuration stood out by achieving a substantial reduction in BD, suggesting its potential suitability for minimizing soil compaction. Conversely, Group B NPTs displayed higher vertical stiffness than PTs, with the M3-6 configuration particularly notable for its effectiveness in reducing BD despite the higher stiffness. These outcomes underscore the intricate interplay between NPT design parameters and their influence on soil productivity. The findings highlight the importance of optimizing NPT design to balance vertical stiffness and soil compaction for agricultural applications.

Future research should consider adopting advanced analytical tools, such as artificial neural networks (ANNs), to further refine NPT configurations. These methodologies could enhance the understanding of the multifaceted relationships between NPT structures and soil interaction, ultimately paving the way for designs that cater to a broader range of agricultural needs. This optimization would contribute to improved efficiency and sustainability in modern farming practices.

8. ACKNOWLEDGMENTS

The authors would like to gratefully acknowledge the Laboratory of Computer Mechanics for Design (LCMD), Department of Mechanical Engineering, Faculty of Engineering, Mahidol University for supporting this research.

9. REFERENCES

- [1] Hamza M. A., and Anderson W. K., Soil Compaction in Cropping Systems a Review of the Nature, Causes and Possible Solutions. *Soil and Tillage Research*, Vol. 82, 2005, pp.121-145.
- [2] Ewa A. C., Effects of Traffic on Soil Aeration, Bulk Density and Growth of Spring Barley. *Soil and Tillage Research*, Vol. 79, 2004, pp.153-166.
- [3] Laclau P. B., and Laclau J. P., Growth of the Whole Root System for a Plant Crop of Sugarcane under Rainfed and Irrigated Environments in Brazil. *Field Crops Research*, Vol. 114, 2009, pp.351-360.
- [4] Patel S. K., Mani I., and Sundaram P. K., Effect of Subsoil Compaction on Rooting Behavior and Yields of Wheat. *Journal of Terramechanics*, Vol. 92, 2020, pp.43-50.
- [5] Obour P. B., and Ugarte C. M., A Meta-Analysis

- of the Traffic-Induced Compaction on Soil Physical Properties and Grain Yield. *Soil and Tillage Research*, Vol. 211, 2021, 105019.
- [6] Botta G. F., Becerra A. T., and Touen F. B., Effect of the Number of Tractor Passes on Soil Rut Depth and Compaction Two Tillage Regimes. *Soil and Tillage Research*, Vol. 103, Issue 2, 2009, pp.381-386.
- [7] Patel S. K., and Mani I., Effect of Multiple Passes of Tractor with Varying Normal Load on Subsoil Compaction, *Journal of Terramechanics*, Vol. 48, 2011, pp.277-284.
- [8] Esteban D. A. A., Souza Z. M., Silva R. B., Souza L. E., Lovera L. H., and Oliveira I. N., Impact of Permanent Traffic Lanes on the Soil Physical and Mechanical Properties in Mechanized Sugarcane Fields with the Use of Automatic Steering, *Geoderma*, Vol. 362, 2020, 114097.
- [9] Farhadi P., Golmohammadi A., Malvajerdi A. S., and Shahgholi G., Finite Element Modeling of the Interaction of a Treaded Tire with Clay-Loam Soil. *Computers and Electronics in Agriculture*, Vol. 162, 2019, pp.793-806.
- [10] Cueto O. G., Coronel C. E. I., Bravo E. L., Morfa C. A. R., and Suarez M. H., Modelling in FEM the Soil Pressure Distribution Caused by a Tyre on Rhodic Ferralsol Soil, *Journal of Terramechanics*, Vol. 63, Issue 1, 2016, pp.61-67.
- [11] Aboulyazid A., Watany M., and Abd Elhafiz M. M., Theoretical Investigation of Spokes Geometry of Non-Pneumatic Tires for Off-Road Vehicles, *SAE Technical Paper 2021-01-0331*, 2021.
- [12] Sidhu C. S., El-Sayegh Z., and Ly A., Non-Pneumatic Tire-Mars Soil Interaction using Advanced Computational Techniques. *SAE Technical Paper 2023-01-0022*, 2023.
- [13] Rugsaj R., and Suvanjumrat C., Revolutionizing Tire Engineering: Finite Element Analysis and Design of an X-Shaped Spoke Structure for Non-Pneumatic Military Tires, *Alexandria Engineering Journal*, Vol. 99, 2024, pp.303-318.
- [14] Suvanjumrat C., and Rugsaj R., The Dynamic Finite Element Model of Non-Pneumatic Tire under Comfortable Riding Evaluation, *International Journal of GEOMATE*, Vol. 19, Issue 76, 2023, pp.62-98.
- [15] Phromjan J., and Suvanjumrat C., Non-Pneumatic Tire with Curved Isolated Spokes for Agricultural Machinery in Agricultural Fields: Empirical and Numerical Study, *Heliyon*, Vol. 9, 2023, e18984.
- [16] Phromjan J., and Suvanjumrat C., Development of spoke structure for agricultural non-pneumatic tire based on the decrease in soil compaction, *Mechanics Based Design of Structures and Machines*, Vol. 53, Issue 1, 2025, pp. 119-148.
- [17] Ju J., Ananthasayanam B., Summer J.D., and Joseph P., Design of Cellular Shear Bands of a Non-Pneumatic Tire Investigation of Contact Pressure, *SAE International Journal of Passenger Cars-Mechanical Systems*, Vol. 3, Issue 1, 2010, pp.598-606.
- [18] Phromjan J., and Suvanjumrat C., Belt Layer Effects on Non-Pneumatic Tire Performance by Finite Element Analysis, In: Agarwal, R.K. (eds) *Recent Advances in Manufacturing Engineering and Processes*. ICMEP 2021. *Lecture Notes in Mechanical Engineering*. Springer, Singapore, 2023, pp.149-157.
- [19] He R., Sandu C., Khan A. K., Guthrie A. G., Els P. S., and Hamersma H. A., Review of Terramechanics Models and their Applicability to Real-Time Applications, *Journal of Terramechanics*, Vol. 81, 2019, pp.3-22.
- [20] Phromjan J., and Suvanjumrat C., Effects on Spoke Structure of Non-Pneumatic Tires by Finite Element Analysis, *International Journal of Automotive Technology*, Vol. 23, Issue 5, 2022, pp.11437-1450.
- [21] Phakdee S., and Suvanjumrat C., Development of a Tire Testing Machine for Evaluating the performance of Tractor Tires Based on the Soil Compaction. *Journal of Terramechanics*, Vol. 110, 2023, pp.13-25.
- [22] Tiwari V. K., Pandey K. P., and Pranav P. K., A Review on Traction Prediction Equations, *Journal of Terramechanics*, Vol. 47, 2010, pp.191-199.
- [23] Phakdee S., Phromjan J., Rugsaj R., and Suvanjumrat S., Experimental Verification of Mathematical Models for Tire-Soil Interaction, *International Journal of GEOMATE*, Vol. 26, Issue 113, 2023, pp.58-95.
- [24] Mukhopadhyay S., Masto R. E., Tripathi R. C., and Srivastava N. K., Chapter 14 – Application of Soil Quality Indicators for the Phytorestoration of Mine Spoil Dumps. In: Pandey, V. C., and Baudhdh, K., editors. *Phytomanagement of Polluted Sites*. Amsterdam: Elsevier; 2019. pp. 361-388.